remote sensing

MDPI

Article

Revealing Annual Crop Type Distribution and Spatiotemporal Changes in Northeast China Based on Google Earth Engine

Yaqun Liu [1,2] and Jieyong Wang [1,2,*]

[1] Institute of Geographic Sciences and Natural Resources Research, Chinese Academy of Sciences, Beijing 100101, China
[2] Key Laboratory of Regional Sustainable Development Modeling, Chinese Academy of Sciences, Beijing 100101, China
* Correspondence: wjy@igsnrr.ac.cn

Abstract: Northeast China (NEC) produces 1/4 of the grain and 1/3 of the commercial grain in China, and is essential for food security and a sustainable socio-ecological system development. However, long-term annual crop type distribution in this vital area remains largely unknown, compromising the scientific basis for planting structure adjustment and sustainable agriculture management. To this end, we integrated 111-dimensional MOD09A1 features, feature optimization and random forest algorithms on the Google Earth Engine (GEE) platform to classify annual crop types in the NEC during 2000–2020, and adopted multi-source spatial data and geostatistical methods to reveal anthropogenic and natural characteristics of crop type changes. The results demonstrated that sample-based classification accuracies were 84.73–86.93% and statistics-based R^2 were 0.81–0.95. From 2000–2020, the sowing area of maize and rice increased by 11.92 $\times$ 10^6 ha (111.05%) and 4.03 $\times$ 10^6 ha (149.28%), whereas that of soybean and other crops decreased by 13.73 $\times$ 10^6 ha (−64.10%) and 1.03 $\times$ 10^6 ha (−50.94%), respectively. Spatially, maize expanded northwestward, rice expanded northeastward, and soybean demonstrated a south-north shrinkage. The soybean-to-maize shift was the main conversion type, and its area largely reduced from 8.68 $\times$ 10^6 ha in 2000–2010 to 4.15 $\times$ 10^6 ha in 2010–2020. Economic comparative benefit and climate change jointly affected crop types in NEC. Higher-benefits maize and rice were mainly planted in more convenient areas with more population and closer to settlements, roads and waterways. The planting of maize and rice required higher temperature and precipitation, and climate change in the NEC provided favorable conditions for their expansion toward high-latitude areas. The crop type changes in the NEC have boosted economic benefits, but increased water–carbon–energy costs. Thus, effective measures such as subsidy policies, ecological compensation, and knowledge-exchange should be implemented to aid crop type and rotation adjustment and ensure food-ecological security.

Keywords: annual crop classification; remote sensing; multi-dimensional features; recursive feature elimination; random forest; Google Earth Engine; sustainable agriculture development

check for updates

Citation: Liu, Y.; Wang, J. Revealing Annual Crop Type Distribution and Spatiotemporal Changes in Northeast China Based on Google Earth Engine. *Remote Sens.* **2022**, *14*, 4056. https://doi.org/10.3390/rs14164056

Academic Editors: Jianxi Huang and Piero Toscano

Received: 13 July 2022
Accepted: 15 August 2022
Published: 19 August 2022

1. Introduction

Cropland is fundamental for food security and sustainable socio-ecological system development, supplying essential goods (e.g., food, feed, fiber, and fuel) and ecosystem services (e.g., carbon sequestration, climate regulation, and biodiversity maintenance) for human society [1–3]. Global population and economic growth have risen the demand for food, causing cropland intensification and expansion [4,5]. Moreover, rapid urbanization and industrialization have consumed a large amount of high-quality cropland [5–7], and climate changes have increased the risk to agricultural production [8]. Thus, scientific crop type distribution and plantation are urgently needed to adapt to the changing environment and to mitigate water consumption, greenhouse gas emissions, and soil quality decline [9–13]. Timely and reliable crop type classification map is the basis for optimizing planting structure and reducing these negative impacts of cropland use.

The commonly used methods to obtain crop type distribution include statistics and remote sensing (RS) [14,15]. However, statistical data has shortcomings such as having low spatial resolution, and being time-consuming and labor-intensive, which make it difficult to timely obtain fine-resolution spatiotemporal distribution information of crop types [14]. By virtue of the ability to provide large-scale, real-time, accurate, and consistent ground information, RS has been widely used in crop classification studies. Many related research projects and platforms have been carried out worldwide. For example, the Large Area Crop Inventory Experiment (LACIE) [16], the Agriculture and Resources Inventory Surveys through Aerospace Remote Sensing (AgRISTARS) [17], and the Cropland Data Layer (CDL) in the United States [18]; the Monitoring Agricultural ResourceS (MARS) project in the European Union; the Annual Crop Inventory (ACI) in Canada [19]; the GEO Global Agricultural Monitoring (GeoGLAM) in the Group of Twenty (G20) [20]; the Crop Monitoring System of Meteorological Bureau, the RS-based Crop Yield Estimation System of Ministry of Agriculture, and the CropWatch system in China [21].

Developments in RS technology have improved the temporal, spatial, spectral, radiometric resolutions, and image computing capabilities. Crop classification platforms have improved from local low-performance software to cloud-based big data platforms such as Google Earth Engine (GEE) and Pixel Information Expert Engine (PIE-Engine) [22,23]. The GEE cloud platform provides multiple open-access RS datasets (e.g., MODIS, Landsat, and Sentinel images), widely-used algorithms (e.g., cloud functions, models, and classifiers), and high-performance computing ability, which makes large-scale and long-term crop classification cost-, labor-, and time-efficient [22,24,25]. The GEE enables individual-produced code and data be open-source and reusable for all researchers, which is beneficial for the improvement of related studies [24,25]. Moreover, classification algorithms have upgraded from traditional unsupervised and supervised methods to machine learning (e.g., random forest, support vector machine, and CART) and deep learning (e.g., CNN, RNN, and GANs) [26,27]. Classification features have developed from single one or a few features to multi-dimensional spectral, spatial, and temporal features [26,28]. However, not all features are useful for classification, and incorporating redundant features may reduce accuracy. The optimal selection feature has become the key to improving classification accuracy [29,30]. In addition, historical crop samples are difficult to obtain, which limits long-term crop classification studies [31]. The lack of annual crop classification studies has led to difficulties in accessing fine-time-interval change characteristics of crop types and rotations [32]. Therefore, it is urgent to classify annual crop types by optimizing multi-dimensional RS features on big data cloud platform, providing the scientific basis for rationalizing crop structure and distribution.

Previous studies have analyzed the spatial distribution, changes, and drivers of crop types in China. Statistical-based analysis found that the sowing proportion of grain crops has declined whereas that of cash crops has increased in China in recent decades [15,33]. The sowing center of grain crops has moved northward, and the area of maize increased significantly whereas that of rice and wheat decreased [4,34]. These changes in crop types and patterns were jointly influenced by anthropogenic (e.g., economic benefits, policies, labor, technology, and dietary structure) and natural factors (e.g., temperature, precipitation, sunlight, soil, and topography) [10,14,33–35]. Cash crops had higher comparative benefits than grain crops and were therefore favored by farmers [14,33]. Economic growth and rising living standards have caused the increased demand for cash crops but decreased demand for grain crops [33,34]. The off-farm transfer and rising costs of rural labors have driven farmers to plant higher-benefits (e.g., cash crops) or easier-mechanization crops (e.g., maize) [14,36]. Natural conditions of climate, soil, and topography limit crop types and planting area, but the improvement of agricultural technologies such as mulch, sprinkler irrigation, drip irrigation, and terrace construction can help overcome these limitations [37,38]. Besides, global warming has expanded the crop-planting area to higher latitudes and altitudes, providing favorable conditions for the northward shift of grain planting center in China [34,39,40]. In general, previous studies have analyzed the characteristics and drivers of crop type changes from different

perspectives, but most of them were based on statistical data, which were difficult to reveal fine-resolution information and support spatially differentiated decision-making. Therefore, it is critical to integrate RS images and spatial raster data of anthropogenic and natural factors to reveal fine-resolution information on crop type distribution, change characteristics, and driving mechanisms.

Northeast China (NEC) produces 1/4 of the grain and 1/3 of the commercial grain, and is one of the most important grain production bases in China [28,41]. In the context of northward shift in China's grain center, the NEC has become more important to national food security [34]. Driven by economic benefits, climate warming, mechanization, rural–urban migration and other factors, the maize and rice in the NEC has expanded significantly, and the grain planting area has been shifted northward [39,42]. However, in recent years, grain production in the NEC has faced challenges such as the decrease in rural labors, climate warming and drying, and degradation of black soil [43–45]. Thus, in the context of human-land system change, exploring the spatiotemporal change characteristics and driving mechanisms of crop types in the NEC is essential for the national strategies of food security as well as black soil conservation and utilization. To this end, based on the GEE big data platform and MODIS MOD09A1 images, we used feature optimization and machine learning algorithms to map the annual spatial distribution of maize, rice, and soybean in the NEC from 2000–2020. We then integrated multi-source spatial data of anthropogenic and natural factors to reveal the change characteristics, and provided policy recommendations for crop planting structure adjustment and sustainable agriculture management.

2. Materials

2.1. Study Area

The NEC has an area of 1.24×10^6 km^2, covering three provinces of Heilongjiang, Jilin, and Liaoning and four eastern leagues of the Inner Mongolia autonomous region (115.52°–135.09°E, 38.72°–53.56°N) (Figure 1). The NEC is one of the four major black soil regions in the world, accounting for about 12% of the total area of the world's total black soil area. The area of NEC cropland in 2020 was about 3.75×10^5 km^2, with concentrated and continuous fields, fertile soil, suitable climate, and high mechanization level. Constrained by the accumulated temperature, crops in the NEC are only one-season. The major grain crops are maize, rice, and soybean, accounting for more than 90% of the crop sowing area in the NEC [28]. The NEC produced about 41%, 19%, and 56% of the national yields of maize, rice, and soybean respectively, making it the most important strategic grain production base in China.

2.2. Data Sources

The multi-source data used in this study included RS images, land use, crop samples, climate, topography, and statistical data. The annual MODIS MOD09A1 products in 2000–2020 were from the NASA LP DAAC (https://lpdaac.usgs.gov/, accessed on 20 November 2021), with the spatial and temporal resolution of 500 m and 8 d, respectively [46]. The data contained 7 bands, and were used to calculate spectral, spatial, and temporal image features for crop classification on the GEE platform.

The 100-m resolution per 5-years land use data in 2000–2020 were from the Resource and Environmental Science and Data Center of the Chinese Academy of Sciences (www.resdc.cn, accessed on 15 September 2021). The data were based on the visual interpretation of Landsat images, with an overall accuracy above 90% [47]. We used this dataset to mask non-cropland land use types and to reduce their interference.

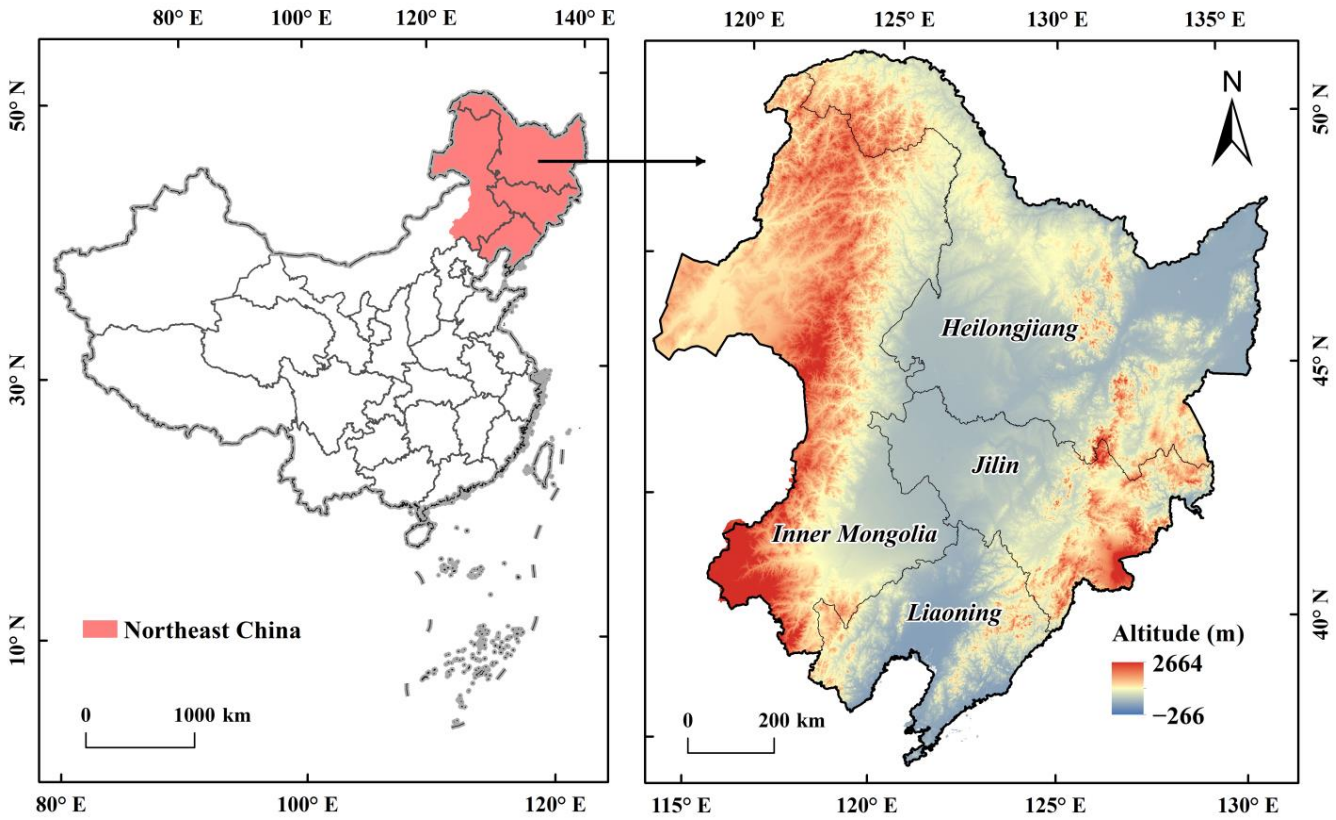

Figure 1. Location and altitude of Northeast China. The vector boundary data of China and Northeast China are from the Resource and Environmental Science and Data Center of the Chinese Academy of Sciences (www.resdc.cn, accessed on 20 November 2021), and the altitude was obtained from the SRTM DEM data (https://srtm.csi.cgiar.org/, accessed on 20 November 2021).

The crop samples were from the 10-m resolution crop type maps in the NEC during 2017–2019 [28]. The dataset was produced based on Sentinel-2 time series data and the GEE platform, with the overall accuracies spanning from 81% to 86%. The classified crop types in this dataset included maize, rice, soybean, and other crops. We randomly selected 3000 pure-pixel samples for each year (specifically, 1467, 1564, and 1521 for maize; 513, 503, and 515 for rice; 861, 785, and 823 for soybean; and 159, 148, and 141 for other crops in 2017, 2018, and 2019, respectively), of which 50% were used for training and classification, and the remaining 50% were used for accuracy validation.

The 30-m resolution topography data of altitude, slope, and aspect were calculated based on the SRTM DEM data (https://srtm.csi.cgiar.org/, accessed on 20 November 2021) [48], which were used for crop classification and distribution pattern analysis.

The 1-km resolution of soil organic carbon (SOC) map was from the dataset of basic soil property dataset of high-resolution China Soil Information Grids (2010–2018) [49], which was used to analyze crop type change characteristics.

The 100-m resolution annual population density data in 2000–2020 were from the WorldPop program (www.worldpop.org, accessed on 17 August 2021), and were used to reveal crop type distribution.

The vector data of settlements, roads and waterways were from the OpenStreetMap (http://download.geofabrik.de/asia/china.html, accessed on 17 August 2021), and were used to calculate the 500-m resolution data of distance to settlements, distance to roads, and distance to waterways for crop type analysis.

The municipal-level statistical data of annual crop sowing area were from provincial statistical yearbooks [50–52], and were used for accuracy assessment.

3. Methods

In this study, we first extracted multi-dimensional spectral, temporal, spatial, and topographic features based on the GEE platform and MOD09A1 data (Figure 2). We then used the recursive feature elimination (RFE) algorithm to optimally select RS features for random forest classification. Finally, we integrated anthropogenic and natural data to reveal the change characteristics and driving mechanism of crop types.

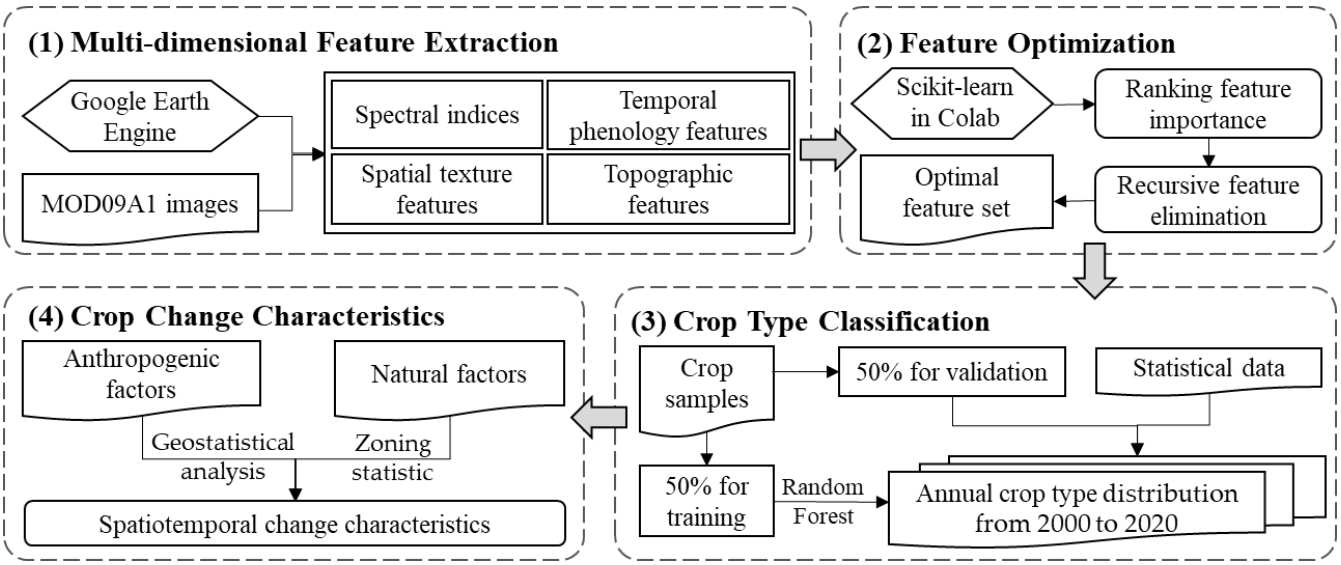

Figure 2. Framework for crop type classification and change characteristics analysis.

3.1. Multi-Dimensional Features' Extraction

The multi-dimensional RS features used for crop type classification included spectral indices, temporal phenology features, spatial texture features, and topographic features.

(1) Spectral indices. We calculated 9 commonly used spectral indices on the GEE platform, including Normalized Difference Vegetation Index (NDVI) [53], Enhanced Vegetation Index (EVI) [54], Normalized Difference Water Index (NDWI) [55], Land Surface Water Index (LSWI) [56], Normalized Differential Senescent Vegetation Index (NDSVI) [57], Normalized Difference Tillage Index (NDTI) [58], Green Chlorophyll Vegetation Index (GCVI) [59], Modified Soil-adjusted Vegetation Index (MSAVI2) [60], and Normalized Difference Snow Index (NDSI) [61]. Their calculation formulas are as follows:

$$NDVI = (\rho_{nir} - \rho_{red})/(\rho_{nir} + \rho_{red}) \tag{1}$$

$$EVI = [2.5 \times (\rho_{nir} - \rho_{red})]/(\rho_{nir} + 6 \times \rho_{red} - 7.5 \times \rho_{blue} + 1) \tag{2}$$

$$NDWI = (\rho_{green} - \rho_{nir})/(\rho_{green} + \rho_{nir}) \tag{3}$$

$$LSWI = (\rho_{nir} - \rho_{swir1})/(\rho_{nir} + \rho_{swir1}) \tag{4}$$

$$NDSVI = (\rho_{swir1} - \rho_{red})/(\rho_{swir1} + \rho_{red}) \tag{5}$$

$$NDTI = (\rho_{swir1} - \rho_{swir2})/(\rho_{swir1} + \rho_{swir2}) \tag{6}$$

$$GCVI = \rho_{nir}/(\rho_{green} - 1) \tag{7}$$

$$MSAVI2 = 1/2 \times \left[2 \times \rho_{nir} + 1 - (2 \times \rho_{nir} + 1)^2 - 8 \times (\rho_{nir} - \rho_{red})^{1/2}\right] \tag{8}$$

$$NDSI = (\rho_{green} - \rho_{swir1})/(\rho_{green} + \rho_{swir1}) \tag{9}$$

where ρ_{blue}, ρ_{green}, ρ_{red}, ρ_{nir}, ρ_{swir1}, and ρ_{swir2} refer to the reflectance of blue, green, red, near-infrared, short-wave infrared 1 and short-wave infrared 2 bands, respectively, corresponding to the 3rd, 4th, 1st, 2nd, 6th, and 7th bands of the MOD09A1 data.

The growing season of major crops in the NEC was from April to October. We calculated the median, mean, maximum, minimum, and standard deviation values in growing season for these 9 spectral indices, and produced 45-dimensional spectral features (Table 1).

Table 1. Multi-dimensional RS features for crop type classification.

Feature Types	Metrics	Periods	Calculation	Dimensions
Spectral Indices	NDVI, EVI, NDWI, LSWI, NDSI, NDSVI, NDTI, GCVI, MSAVI2	Growing season	Median, mean, maximum, Minimum, standard deviation	$9 \times 1 \times 5 = 45$
Temporal Phenology Features		Seeding stage, growth stage, harvest stage	median	$9 \times 3 \times 1 = 27$
Spatial Texture Features	NDVI, LSWI	Growing season	Median and GLCM	$2 \times 1 \times 18 = 36$
Topographic Factors		Elevation, slope, aspect		3

(2) Temporal phenology features. We used the 90th (April 1) day of year (DOY) as starting date and 64 days as time intervals to divide the growing season into 3 phenology periods, i.e., seeding (DOY of 90–154), growth (154–218), and harvest stages (218–282). We calculated the median values in 3 phenology periods for 9 spectral indices to obtain 27-dimensional temporal phenology features.

(3) Spatial texture features. In this study, we adopted the Gray Level Co-occurrence Matrix (GLCM) transform, a commonly used method based on the spatial correlation relationships of image pixel brightness values (grey levels), to extract spatial texture features [26,62]. The GLCM transform was performed based on 18 metrics (i.e., angular second moment, contrast, correlation, variance, inverse difference moment, sum average, sum variance, sum entropy, entropy, difference variance, difference entropy, information measures of correlation 1 and correlation 2, max correlation coefficient, dissimilarity, inertia, cluster shade, and cluster prominence) for the median values of NDVI and LSWI to generate 36-dimensional spatial texture features.

(4) Topographic features. We also calculated the topographic features of altitude, slope, and aspect based on the SRTM DEM data [63] for crop type classification, due to these factors affecting farmers' planting choices of crop types to a certain extent.

3.2. Feature Optimization Selection

(1) Ranking feature importance. We integrated 111-dimensional spectral, temporal, spatial, and topographic features, and calculated and ranked their Gini importance coefficients (Figure 3). The feature importance of LSWI, NDSI, and NDSVI were relatively high, and the mean LSWI value in growing season had the highest importance. However, the importance of low-ranked features were only one-fifth of the highest value. Thus, for more effective and accurate feature selection, we removed low-importance features and retained approximately half of (55-dimensional) the features.

(2) Recursive feature elimination (RFE). The RFE algorithm is a feature selection method that recursively removes the least important feature until it reaches the desired number of features [64]. In this study, we used the RFE algorithm with cross-validation (RFECV) of scikit-learn package in the Google Colab platform to select the optimal feature set from 55-dimensional features. The RFECV algorithm uses an automatic tuning cross-validation loop to find the optimal number of features. Figure 4 showed the validation accuracies for different number of feature sets, and the optimal number of features was determined as 23 with highest cross-validation accuracy. Thus, we finally adopted 23-dimensional optimal features for crop type classification.

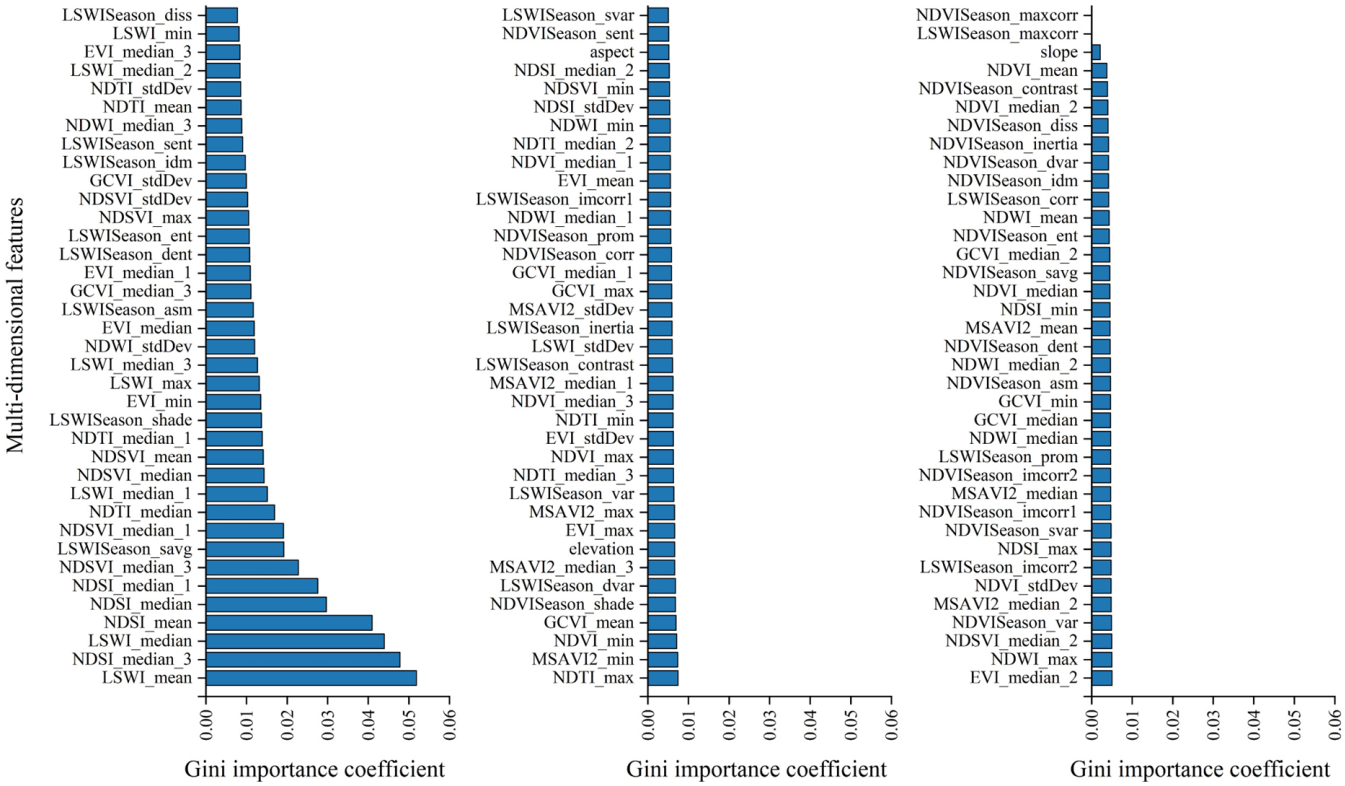

Figure 3. Ranking Gini importance coefficients of 111-dimensional spectral, temporal, spatial, and topographic features.

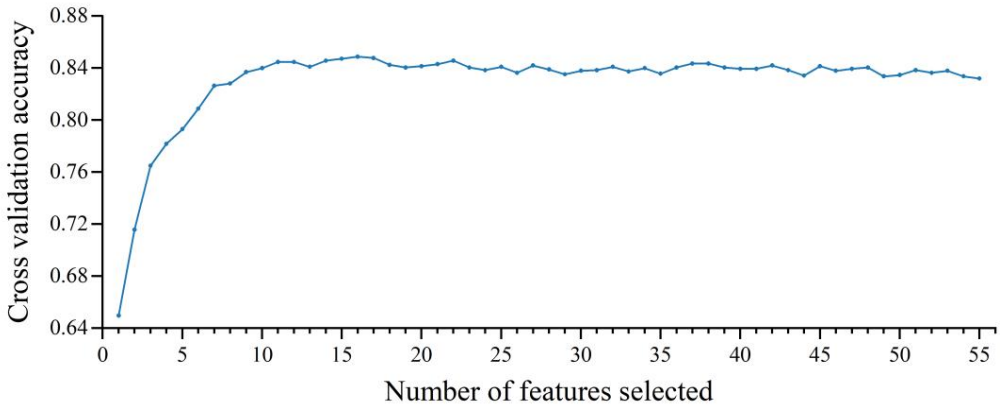

Figure 4. Recursive feature elimination of 55-dimensional features.

3.3. Random Forest for Annual Crop Classification

Random forest (RF) is a widely used Bagging algorithm of ensemble learning containing multiple decision trees [28,30], which improves the accuracy and stability of classification by training multiple models to reduce generalization error and avoid overfitting. Although RF has the ability to resist noise and deal with high-dimensional data, introducing too many invalid features can still lead to overfitting [30]. Therefore, feature optimization selection is necessary for RF-based crop classification of high-dimensional data. In this study, we used the RF algorithm with 500 decision trees to classify crop type based on the 23-dimensional optimal features on the GEE platform.

In this study, we used the crop samples in 2017–2019 to conduct annual crop type classification during 2000–2020. Specifically, we first carried out the 2019 crop classification, and then used the 2019 RF classifier with satisfactory accuracy to classify the 2017 and 2018

crop types, and evaluated their classification accuracies based on samples. After proving that the year-specific classifier can be used effectively for the classifications of other years, we classified annual crop types for other years during 2000–2020 based on the 2019 classifier, and assessed their classification accuracies using statistical yearbook data.

3.4. Analysis of Crop Type Change Characteristics

The distribution and change of different crop types are jointly influenced by anthropogenic (e.g., economic benefits, policies, labor, and technology) and natural factors (e.g., climate, soil, and topography) [14,33]. Thus, revealing the spatiotemporal change characteristics of crop types can help understanding the underlying causes. In this study, we used the geostatistical methods [65] in the ArcGIS 10.8 software (Environmental Systems Research Institute, Redlands, CA, USA) to analyze the crop type, area, and their changes and conversions in the NEC during 2000–2020. In addition, by integrating the factors of population density, distance to settlements, distance to roads, distance to waterways, precipitation, temperature, soil organic carbon (SOC), altitude, and slope, the buffering, overlay, and zoning statistics were used to reveal the anthropogenic and natural characteristics of crop type changes.

4. Results

4.1. Classification Accuracy Assessment

Confusion matrix-based accuracy assessment found an overall accuracy of 86.93% and a Kappa coefficient of 0.79 for the 2019 crop type classification (Table 2). Using the 2019 classifier to map the crop types in 2017 and 2018, the overall accuracies were 86.33% and 84.73%, and Kappa coefficients were 0.78 and 0.76, respectively. In terms of crop types, rice had the highest accuracy, and other crops had the lowest accuracy. The misclassification between maize and soybean was relatively high due to their close growing seasons.

Table 2. Confusion matrix between crop type classification result and validation samples.

Crop Types		Validation Samples in 2019					User Accuracy (%)
		Maize	Rice	Soybean	Other Crops	Total	
Classification Result in 2019	Maize	696	12	82	4	794	87.66
	Rice	15	239	6	0	260	91.92
	Soybean	49	9	315	6	379	83.11
	Other Crops	5	3	5	54	67	80.60
	Total	765	263	408	64	1500	
Mapping Accuracy (%)		90.98	90.87	77.21	84.38		
Crop Types		**Validation Samples in 2018**					**User Accuracy (%)**
		Maize	**Rice**	**Soybean**	**Other Crops**	**Total**	
Classification Result in 2018	Maize	703	21	70	5	799	87.98
	Rice	17	218	4	3	242	90.08
	Soybean	61	4	299	1	365	81.92
	Other Crops	9	4	6	75	94	79.79
	Total	790	247	379	84	1500	
Mapping Accuracy (%)		88.99	88.26	78.89	89.29		
Crop Types		**Validation Samples in 2017**					**User Accuracy (%)**
		Maize	**Rice**	**Soybean**	**Other Crops**	**Total**	
Classification Result in 2017	Maize	652	18	78	11	759	85.90
	Rice	11	223	13	2	249	89.56
	Soybean	57	8	335	7	407	82.31
	Other Crops	5	9	10	61	85	71.76
	Total	725	258	436	81	1500	
Mapping Accuracy (%)		89.93	86.43	76.83	75.31		

Note: Overall accuracies were 86.93%, 86.33%, and 84.73%, and Kappa coefficients were 0.79, 0.78, and 0.76 in 2019, 2018, and 2017, respectively.

We compared a municipal-level statistical data of crop area with annual mapped area, and found that their coefficient of determination (R^2) values were 0.81–0.95 (Figure 5). The R^2 values were the lowest in 2001, 2003, 2005, and 2010, and the highest in 2015. Further analysis found that the crop classification in more recent years had higher R^2 values with statistical area than earlier years (2000–2005), indicating that the 2019 classifier performed better for optimized features in recent years. This may be due to the impacts of climate variations, seed shift, and field management changes on crop growth. In addition, the areas of mapped different crops were mainly larger than statistical area, implying that the statistics may miss part of the crop distributions.

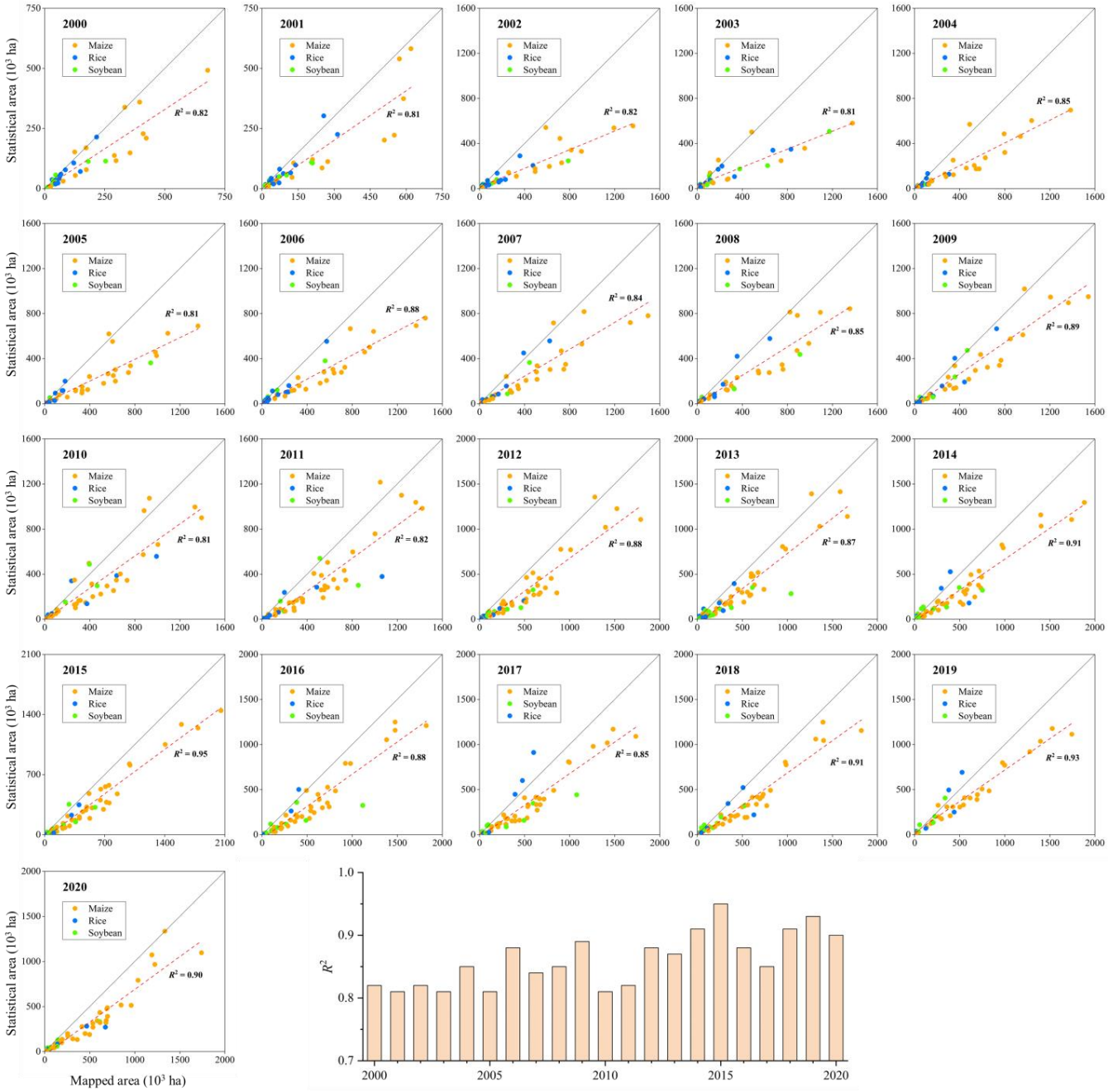

Figure 5. Comparison of annual mapped crop area and municipal-level statistical area in the NEC from 2000 to 2020.

4.2. Annual Crop Type Distribution and Area Changes

The crop type distribution demonstrated significant spatial heterogeneity in the NEC from 2000 to 2020 (Figure 6). In 2000, the crop distribution was dominated by soybean, mainly located in the northwest. However, over time, the soybean distribution has shrunk significantly from south to north, while the maize distribution has expanded dramatically towards the northwest. As a result, the maize gradually became the dominated crop, mainly distributed in the southern and central of NEC. In addition, rice was mainly concentrated in the northeast of NEC, showing a trend of expansion. Other crops were distributed scattered, with relatively low variation.

From 2000 to 2020, the most significant changes in crop types in the NEC were the expansion of maize and rice, and the shrinkage of soybean and other crops (Figure 7). The sowing area of maize and rice increased from 10.74×10^6 ha and 2.70×10^6 ha to 22.66×10^6 ha and 6.73×10^6 ha, increased by 11.92×10^6 ha (111.05%) and 4.03×10^6 ha (149.28%), respectively. Conversely, that of soybean and other crops decreased from 21.42×10^6 ha and 2.01×10^6 ha to 7.69×10^6 ha and 0.99×10^6 ha, decreased by 13.73×10^6 ha (−64.10%) and 1.03×10^6 ha (−50.94%), respectively. Moreover, the maize area increased rapidly in 2002, while soybean area fell sharply. After 2015, the maize area demonstrated a slight decrease, whereas soybean demonstrated an increasing trend. In addition, the area proportion of maize and rice increased from 29.12% and 7.32% in 2000 to 59.53% and 17.67% in 2012, respectively. However, the proportion of soybean and other crops decreased from 58.10% and 5.46% to 20.20% and 2.60%, respectively.

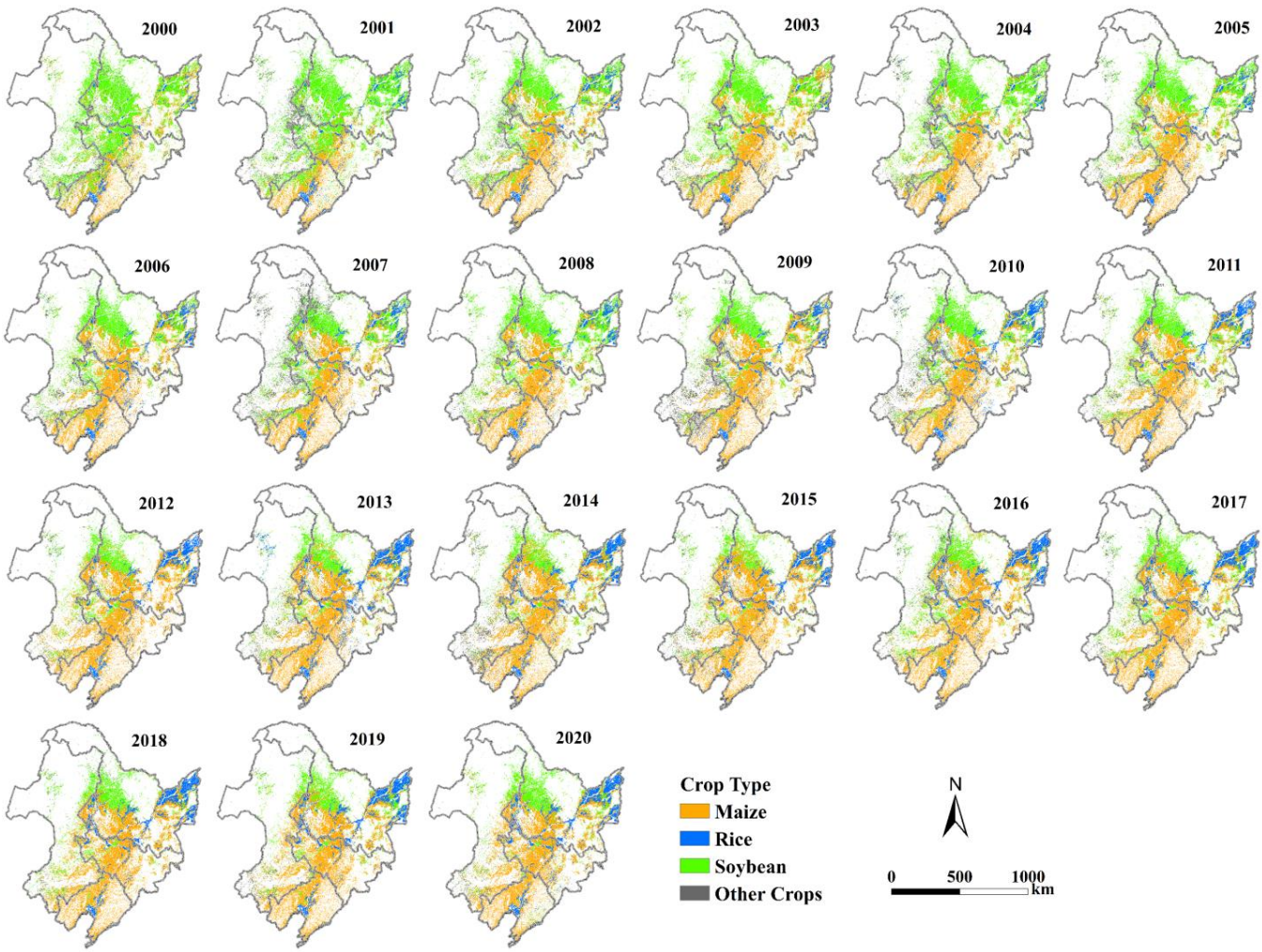

Figure 6. Annual crop type distribution in the NEC from 2000 to 2020.

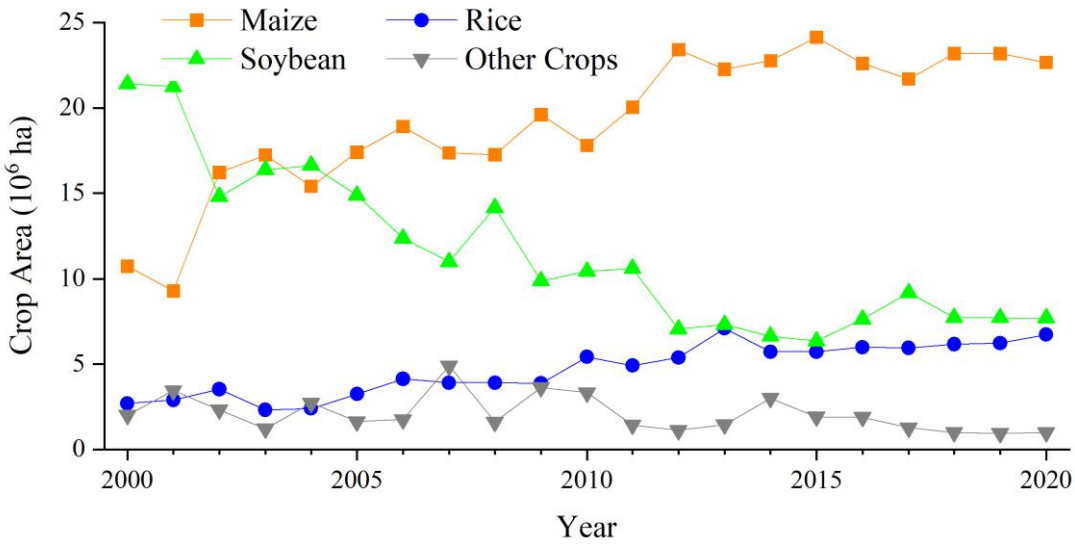

Figure 7. Annual crop area changes in the NEC from 2000 to 2020.

4.3. Spatiotemporal Conversions of Crop Types

From 2000–2010, large amounts of soybean have converted to maize in the central of NEC, mainly located in the Songnen Plain and Liao River Plain (Figure 8). The maize and soybean in the northeast of NEC were largely converted to rice, mainly distributed in the Sanjiang Plain and a few in the Songnen Plain. Furthermore, some of the maize in the Inner Mongolia autonomous region were converted to other crops. From 2010–2020, the converted area of soybean to maize was significantly reduced compared to 2000–2010, and these conversions mainly occurred within Heilongjiang, and near the border between Inner Mongolia and Jilin and Heilongjiang. Most of the expanded rice was converted from maize and soybean distributed within Heilongjiang.

The crop type conversion in NEC was mainly the shift of soybean to maize. From 2000–2010, the area of soybean converted to maize was 8.68 × 10^6 ha, which accounted for 48.73% of the total maize area in 2010 (Table 3). In addition, the areas of maize and soybean converted to rice were 1.68 × 10^6 ha and 1.38 × 10^6 ha, accounting for 31.09% and 25.59% of the total rice area in 2010, respectively. Of the total area of other crops in 2010, 67.13% (2.23 × 10^6 ha) was converted from soybean.

Table 3. Conversion matrix of crop types in the NEC from 2000 to 2020.

		Gains in 2010 (10^6 ha)				
		Maize	**Rice**	**Soybean**	**Other Crops**	**Total**
Losses in 2000 (10^6 ha)	Maize		1.68	0.91	0.30	2.90
	Rice	0.42		0.06	0.04	0.52
	Soybean	8.68	1.38		2.23	12.29
	Other Crops	0.78	0.03	0.48		1.30
	Total	9.88	3.10	1.46	2.57	17.02
		Gains in 2020 (10^6 ha)				
		Maize	**Rice**	**Soybean**	**Other Crops**	**Total**
Losses in 2010 (10^6 ha)	Maize		1.11	0.72	0.07	1.91
	Rice	0.68		0.08	0.01	0.77
	Soybean	4.15	0.50		0.10	4.75
	Other Crops	1.51	0.04	0.86		2.41
	Total	6.35	1.66	1.65	0.18	9.84

From 2010–2020, the converted area of soybean to maize largely reduced compared to 2000–2010, with only 4.15 × 10^6 ha, accounting for 18.32% of the 2020 maize area (Table 3). The increased area of rice from 2010 to 2020 was also mainly from maize and soybean, accounting for 16.57% (1.11 × 10^6 ha) and 7.50% (0.50 × 10^6 ha) of the 2020 rice area, respectively.

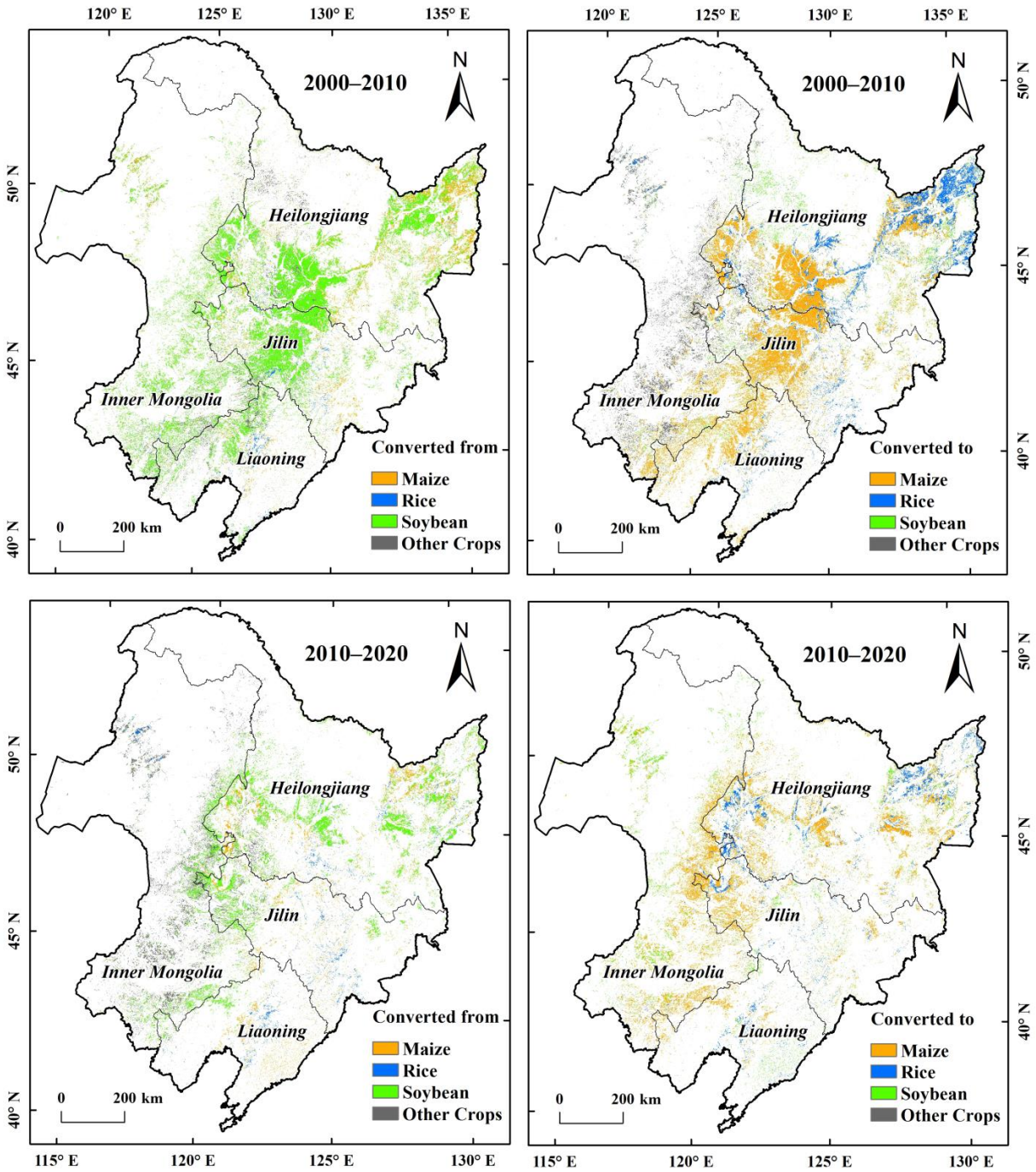

Figure 8. Spatiotemporal crop type conversions in the NEC during 2000–2020.

4.4. Anthropogenic and Natural Characteristics of Crop Type Changes

Geostatistical analysis found significant heterogeneities in the different crop types and their changes (Figure 9). In terms of anthropogenic factors, maize and rice were mainly located in more densely populated areas closer to settlements and roads than soybean and other crops. The type-unaltered areas of different crops during 2010–2020 trended to be

farther from settlements and roads than 2000–2010. Maize expanded closer to settlements and roads during 2000–2010, while expanded farther during 2010–2020. The expanded areas of rice and soybean were farther from settlements and roads than reduced areas from 2000–2020.

In terms of natural factors, maize and rice were closer to waterways than soybean and other crops, and rice was closest due to its highest water requirements. From 2000 to 2020, maize expanded farther from waterways, and soybean reduction was located closer to waterways. Rice expanded nearer to waterways during 2000–2010, whereas its characteristic was reversed during 2010–2020.

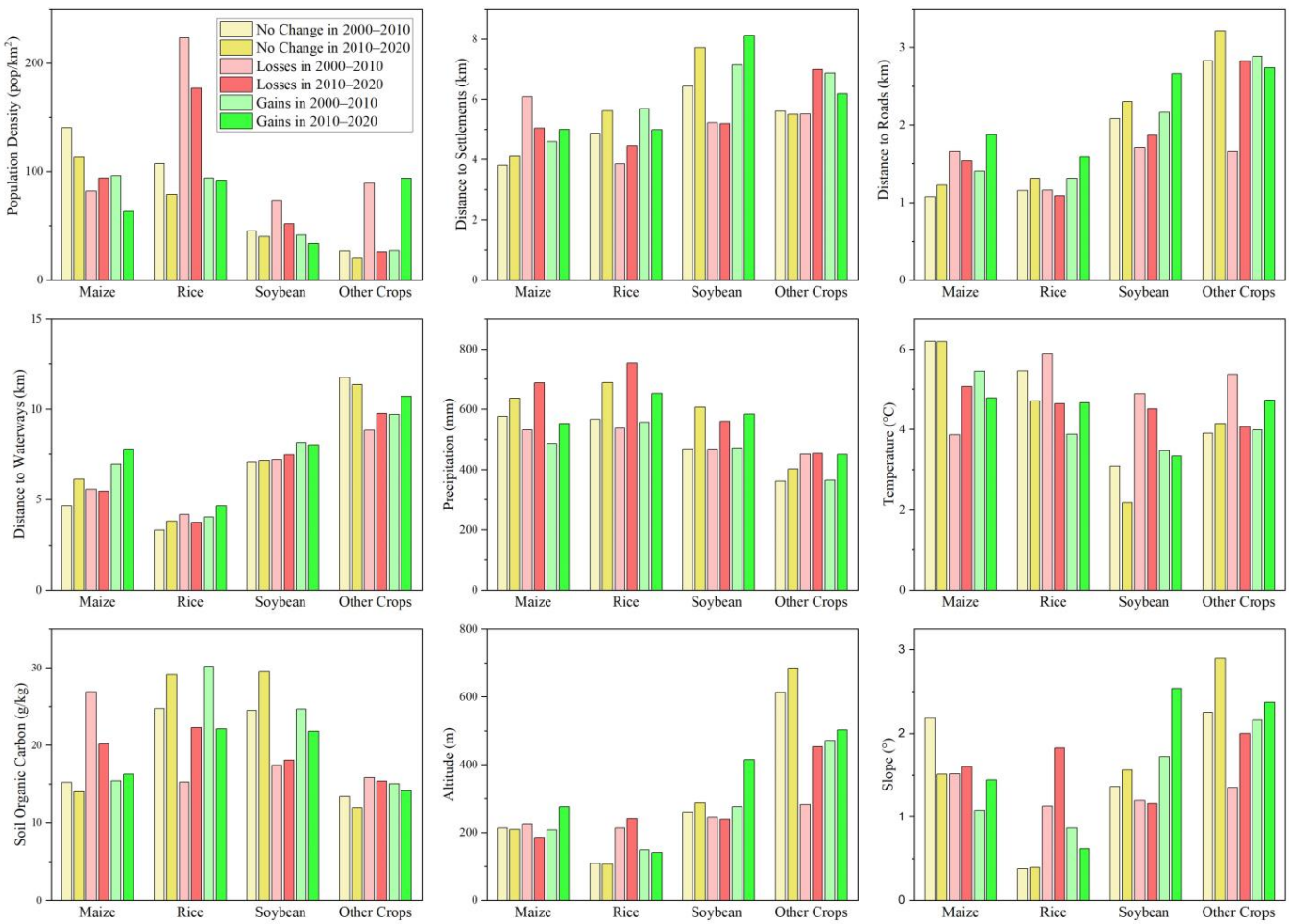

Figure 9. Anthropogenic and natural characteristics of crop type changes in the NEC during 2000–2020.

The distributed areas of maize and rice had relatively higher precipitation and temperature than soybean and other crops. From 2000 to 2020, expanded maize and rice, and reduced soybean were mainly located in lower-precipitation areas. Reduced soybean was mainly in higher-temperature areas. Maize expanded to higher-temperature areas and rice expanded to lower-temperature areas during 2000–2010, while their characteristics were reversed during 2010–2020.

In the type-unaltered areas, the SOC of rice and soybean were significantly higher than that of maize and other crops. Expanded maize and reduced soybean had relatively lower SOC, while expanded rice had higher SOC.

Among major crops, rice had the lowest altitude and smallest slope. From 2000 to 2020, expanded rice and reduced soybean were mainly in lower-altitude and smaller-slope areas. Maize expanded toward lower-altitude and smaller-slope areas during 2000–2010, while toward higher-altitude and smaller-slope areas during 2010–2020. Other crops had

the highest altitude and biggest slope, and were distributed toward higher-altitude and bigger-slope areas.

5. Discussion

5.1. Limitations and Future Improvements of Annual Crop Classification

Most previous studies have identified crop type distribution in recent years with multi-year intervals [14,28,32]. However, long-term annual crop classification studies remain rare due to hard-to-obtain historical samples, which made it difficult to reveal fine-time-interval characteristics of crop type and rotation changes [28]. In the study, we used sample-based classifier with satisfactory accuracy in 2017–2019 to classify the crop types in other years without samples. Although the classification accuracies in no-sample years have satisfactorily assessed by statistical data, the statistics-based R^2 was relatively low in the early years (2000–2005). Previous research found that climate variations over the long-term may affect crop growth status and type classification [32], which was not considered in this study. Future studies can use temporal transfer learning algorithms [66] to generate historical virtual samples and introduce climate factors [32] as key features to classify crop types more accurately.

Among the main crop types in the NEC, rice has its unique growing season, which was significantly different from other crops. The rice phenology was also more sensitive to water index than other crops. As a result, we adopted two commonly used water indices (i.e., NDWI, LSWI) [56], assisted with multiple spectral, temporal, spatial, and topographic features, to classify crop types, and rice was mapped with the highest accuracy. The high performance of LSWI in the crop type classification involving rice was confirmed by our study and previous studies [28,41]. However, the misclassification between maize and soybean was relatively high due to their similar phenology, which was in line with previous research [28]. To better identify these crop types, future studies can add more features (e.g., polarization features from SAR data) with finer time interval to map crop types. Besides, the MOD09A1 products used in this study only has a spatial resolution of 500 m. Although the data was suitable for the NEC with large-area plots, it was too coarse for the areas with fragmented cropland [14]. Indeed, the classification based on higher resolution imagery with finer time interval had a higher accuracy than this study [28]. Thus, fine-resolution RS data such as 30-m Landsat and 10-m Sentinel data are urgently needed for future crop classification [27,28,32]. Moreover, we only used RF algorithm to classify annual crop types, but did not compare its performance with other machine learning algorithms such as SVM and CART. Therefore, future research should compare the accuracies of multiple classifiers to find more stable optimization features and to improve crop classification.

5.2. Potential Applications of GEE-Based Annual Crop Type Distribution

By virtue of open-access datasets, widely-used algorithms, and high-performance computing ability, the GEE cloud platform is cost-, labor-, and time-efficient in producing large-scale and long-term crop type classification [22,24,25,28]. Moreover, individual-produced code and data based on the GEE platform can be open-source and reusable for all researchers [24,25]. Thus, both the code of data processing, feature extraction and selection and classifier setup, and annual crop type classification results in this study were beneficial for the improvement of related studies, which can make some contributions to the RS community.

Crop classification, especially long-term classification, is the basis for understanding the process, pattern, drivers, and economic-ecological effects of crop type distribution and their changes. Compared to crop classification studies with multi-year interval, long-term annual crop classification can provide finer time-interval information on crop type and change trajectories for sustainable agriculture management. Previous studies have mainly revealed crop rotation information based on time-consuming field surveys or observations for consecutive years [67–69]. Moreover, previous studies have analyzed the effects of different crop rotation types on soil organic carbon (SOC) based on field

experiments or observations [68,69]. However, due to the lack of crop rotation map, the critical and fundamental information on fine spatial heterogeneity of these effects remain unknown. Thus, the large-area and long-term spatial distribution of crop rotation and its multidimensional (e.g., yield, carbon, water, and energy) effects are urgently needed to be mapped based on annual crop classification, supporting scientific basis for crop type and rotation optimization.

5.3. Causes, Effects, and Policy Implications of Crop Type Change

Crop type changes are jointly affected by anthropogenic and natural factors [33,34,39,40,70]. Specifically, economic benefits and labor cost were two key anthropogenic factors for the crop type changes in the NEC. With the growth of social economy and labor income, most farmers migrated to cities for off-farm employment, and the remaining farmers preferred to plant higher-benefits or labor-saving crops [70]. Although rice was labor-intensive, it had the highest comparative economic benefits among major crops [14]. Maize had higher comparative benefits and was easier-mechanization than soybean. Thus, the planting area of maize and rice increased, and that of soybean decreased in the NEC, which were consistent with previous studies [28]. Moreover, farmers tend to plant higher-benefits maize and rice in more convenient areas, i.e., the areas closer to settlements, roads, and waterways. In addition, climate change, especially global warming, was the main natural factor for the crop changes of NEC [39]. The planting of maize and rice required a higher accumulated temperature and water requirement than soybean. Thus, maize and rice were mainly located in the areas with higher precipitation and temperature, and climate warming trend provided favorable conditions for maize and rice expansion in high-latitude areas of NEC [39,40].

Although maize and rice have relatively higher economic benefits, they also consume more water, fertilizer, and energy [38]. Thus, the expansion of maize and rice has boosted farmers' incomes, but also increased the costs of water, carbon, and energy consumption in the NEC [50–52]. As a result, groundwater has declined and black soil has been degraded in the NEC over the past few decades [45,71]. In addition, previous studies found that rice was an important emission source of greenhouse gases such as methane (CH_4) and nitrous oxide (N_2O) [72,73]. As soybean have been shown to increase soil nitrogen, it would be better to expand maize in the form of maize-soybean rotation instead of continuous maize [74]. Thus, decision-makers should adopt effective measures such as subsidy policies, ecological compensation, and knowledge-exchange to enhance farmers' awareness of low-carbon planting and guide farmers to practice more environmentally friendly rotation form and field management [3,38]. To achieve food security and sustainable agricultural development, multi-objective optimization and scenario simulation studies should be emphasized on the basis of revealing the process-mechanism-effect of crop type and rotation spatiotemporal changes in the future.

6. Conclusions

In this study, we provided a GEE-based methodological framework to map annual crop type distribution and spatiotemporal change. By integrating multi-dimensional MOD09A1 features, multi-source anthropogenic and natural data, and multiple methods of feature optimization, random forest and geo-statistics, we classified annual crop types with sample-based overall accuracies of 84.73–86.93% and statistics-based R^2 of 0.81–0.95, and revealed anthropogenic and natural change characteristics in the NEC during 2000–2020.

The result demonstrated that maize was mainly planted in the south and central of NEC and expanded northwestward by 111.05%. Rice was concentrated in the northeastern and expanded by 149.28%, whereas soybean was located in the northwestern and showed a south-north shrinkage of –64.10%. Consequently, the proportion of maize and rice increased from 29.12% and 7.32% to 59.53% and 17.67%, while that of soybean and other crops decreased from 58.10% and 5.46% to 20.20% and 2.60%, respectively. The soybean-to-maize shift was the main conversion type, and its area largely reduced from 8.68×10^6 ha in 2000–2010 to 4.15×10^6 ha in 2010–2020, accounting for 48.73% of the 2010 maize area and

18.32% of the 2020 maize area. Higher-benefits maize and rice were mainly planted in more convenient areas with more population and closer to settlements, roads, and waterways. Their planting required higher temperature and precipitation, and climate change in the NEC provided favorable conditions for their expansion toward high-latitude areas. The crop type changes in the NEC have boosted economic benefits, but increased water-carbon-energy costs. Thus, effective measures such as subsidy policies, ecological compensation, and knowledge-exchange should be implemented to ensure food-ecological security. Future studies could focus on multi-objective optimization and scenario simulation to aid crop type, rotation adjustment, and sustainable agriculture management.

Author Contributions: Conceptualization, Y.L. and J.W.; methodology, Y.L.; formal analysis, Y.L; investigation, Y.L.; resources, J.W.; writing—original draft preparation, Y.L.; writing—review and editing, J.W.; supervision, J.W. All authors have read and agreed to the published version of the manuscript.

Funding: This research was supported by the Strategic Priority Research Program of the Chinese Academy of Sciences (Grant No. XDA28130400), the National Natural Science Foundation of China (Grant Nos. 41931293 and 42171266), and the Project funded by China Postdoctoral Science Foundation (Grant No. 2021M700143).

Data Availability Statement: The GEE code for crop type classification in 2019 is available on https://code.earthengine.google.com/76995efc420d1bef4df5b5faaa588b1b. The data presented in this research are available on request from the corresponding author.

Acknowledgments: We greatly appreciate the editors and anonymous reviewers for their valuable time, constructive suggestions, and insightful comments.

Conflicts of Interest: The authors declare no conflict of interest.

References

1. Xiao, X.Y.; Shang, L.X.; Liu, Y.Q. Comparative Study on Farmland Circulation between Plains and Mountainous Areas in an Arid Region: A Case Study of Zhangye City in Northwest China. *Land* **2022**, *11*, 571. [CrossRef]
2. Liu, Y.Q.; Song, W.; Mu, F.Y. Changes in ecosystem services associated with planting structures of cropland: A case study in Minle County in China. *Phys. Chem. Earth* **2017**, *102*, 10–20. [CrossRef]
3. Liu, Y.Q.; Song, W. Mapping human appropriation of net primary production in agroecosystems in the Heihe River Basin, China. *Agric. Ecosyst. Environ.* **2022**, *335*, 107996. [CrossRef]
4. Zhong, H.M.; Liu, Z.J.; Wang, J.Y. Understanding impacts of cropland pattern dynamics on grain production in China: A integrated analysis by fusing statistical data and satellite-observed data. *J. Environ. Manag.* **2022**, *313*, 114988. [CrossRef]
5. Liu, Y.S.; Fang, F.; Li, Y.H. Key issues of land use in China and implications for policy making. *Land Use Policy* **2014**, *40*, 6–12. [CrossRef]
6. Song, W. Decoupling cultivated land loss by construction occupation from economic growth in Beijing. *Habitat Int.* **2014**, *43*, 198–205. [CrossRef]
7. Song, W.; Pijanowski, B.C.; Tayyebi, A. Urban expansion and its consumption of high-quality farmland in Beijing, China. *Ecol. Indic.* **2015**, *54*, 60–70. [CrossRef]
8. Ewert, F.; Rotter, R.P.; Bindi, M.; Webber, H.; Trnka, M.; Kersebaum, K.C.; Olesen, J.E.; van Ittersum, M.K.; Janssen, S.; Rivington, M.; et al. Crop modelling for integrated assessment of risk to food production from climate change. *Environ. Model. Softw.* **2015**, *72*, 287–303. [CrossRef]
9. Liu, Y.Q.; Song, W.; Deng, X.Z. Spatiotemporal Patterns of Crop Irrigation Water Requirements in the Heihe River Basin, China. *Water* **2017**, *9*, 616. [CrossRef]
10. Zhang, Y.; Wang, J.Y.; Dai, C. The Adjustment of China's Grain Planting Structure Reduced the Consumption of Cropland and Water Resources. *Int. J. Environ. Res. Public Health* **2021**, *18*, 7352. [CrossRef]
11. Liu, Z.J.; Liu, Y.S.; Wang, J.Y. A global analysis of agricultural productivity and water resource consumption changes over cropland expansion regions. *Agric. Ecosyst. Environ.* **2021**, *321*, 107630. [CrossRef]
12. Gelybo, G.; Barcza, Z.; Dencso, M.; Potyo, I.; Kasa, I.; Horel, A.; Pokovai, K.; Birkas, M.; Kern, A.; Hollos, R.; et al. Effect of tillage and crop type on soil respiration in a long-term field experiment on chernozem soil under temperate climate. *Soil Tillage Res.* **2022**, *216*, 105239. [CrossRef]
13. Jiang, M.; Li, X.B.; Xin, L.J.; Tan, M.H. Paddy rice multiple cropping index changes in Southern China: Impacts on national grain production capacity and policy implications. *J. Geogr. Sci.* **2019**, *29*, 1773–1787. [CrossRef]
14. Liu, Y.Q.; Song, W.; Deng, X.Z. Changes in crop type distribution in Zhangye City of the Heihe River Basin, China. *Appl. Geogr.* **2016**, *76*, 22–36. [CrossRef]

15. Wu, B.F.; Li, Q.Z. Crop planting and type proportion method for crop acreage estimation of complex agricultural landscapes. *Int. J. Appl. Earth Obs. Geoinf.* **2012**, *16*, 101–112. [CrossRef]
16. Pinter, P.J.; Ritchie, J.C.; Hatfield, J.L.; Hart, G.F. The agricultural research service's remote sensing program: An example of interagency collaboration. *Photogramm. Eng. Rem. Sens.* **2003**, *69*, 615–618. [CrossRef]
17. Houston, A.G.; Hall, F.G. Use of Satellite Data in Agricultural Surveys. *Commun. Stat.-Theor. Methods* **1984**, *13*, 2857–2880. [CrossRef]
18. Boryan, C.; Yang, Z.W.; Mueller, R.; Craig, M. Monitoring US agriculture: The US Department of Agriculture, National Agricultural Statistics Service, Cropland Data Layer Program. *Geocarto. Int.* **2011**, *26*, 341–358. [CrossRef]
19. PERDIGAO, V.; Vossen, P.; Gallego, J. In The Mars project: The European approach adaptable to national needs. In Proceedings of the Workshop on New Tools for Agriculture and Forestry Statistics, Oporto, Portugal, 19–20 October 1995; pp. 63–78.
20. Whitcraft, A.K.; Becker-Reshef, I.; Justice, C.O. A Framework for Defining Spatially Explicit Earth Observation Requirements for a Global Agricultural Monitoring Initiative (GEOGLAM). *Remote Sens.* **2015**, *7*, 1461–1481. [CrossRef]
21. Wu, B.F.; Meng, J.H.; Li, Q.Z.; Yan, N.N.; Du, X.; Zhang, M. Remote sensing-based global crop monitoring: Experiences with China's CropWatch system. *Int. J. Digit. Earth* **2014**, *7*, 113–137. [CrossRef]
22. Gorelick, N.; Hancher, M.; Dixon, M.; Ilyushchenko, S.; Thau, D.; Moore, R. Google Earth Engine: Planetary-scale geospatial analysis for everyone. *Remote Sens. Environ.* **2017**, *202*, 18–27. [CrossRef]
23. Li, J.F.; Wang, L.Y.; Liu, S.Q.; Peng, B.A.; Ye, H.P. An automatic cloud detection model for Sentinel-2 imagery based on Google Earth Engine. *Remote Sens Lett.* **2022**, *13*, 196–206. [CrossRef]
24. Li, H.; Wan, W.; Fang, Y.; Zhu, S.Y.; Chen, X.; Liu, B.J.; Hong, Y. A Google Earth Engine-enabled software for efficiently generating high-quality user-ready Landsat mosaic images. *Environ. Model. Softw.* **2019**, *112*, 16–22. [CrossRef]
25. Zhang, C.; Di, L.P.; Yang, Z.W.; Lin, L.; Hao, P.Y. AgKit4EE: A toolkit for agricultural land use modeling of the conterminous United States based on Google Earth Engine. *Env. Model. Softw.* **2020**, *129*, 104694. [CrossRef]
26. Liu, Y.Q.; Song, W.; Deng, X.Z. Understanding the spatiotemporal variation of urban land expansion in oasis cities by integrating remote sensing and multi-dimensional DPSIR-based indicators. *Ecol. Indic.* **2019**, *96*, 23–37. [CrossRef]
27. Wang, S.; Azzari, G.; Lobell, D.B. Crop type mapping without field-level labels: Random forest transfer and unsupervised clustering techniques. *Remote Sens. Environ.* **2019**, *222*, 303–317. [CrossRef]
28. You, N.S.; Dong, J.W.; Huang, J.X.; Du, G.M.; Zhang, G.L.; He, Y.L.; Yang, T.; Di, Y.Y.; Xiao, X.M. The 10-m crop type maps in Northeast China during 2017–2019. *Sci. Data* **2021**, *8*, 41. [CrossRef]
29. Low, F.; Michel, U.; Dech, S.; Conrad, C. Impact of feature selection on the accuracy and spatial uncertainty of per-field crop classification using Support Vector Machines. *ISPRS J. Photogram.* **2013**, *85*, 102–119. [CrossRef]
30. Hao, P.Y.; Zhan, Y.L.; Wang, L.; Niu, Z.; Shakir, M. Feature Selection of Time Series MODIS Data for Early Crop Classification Using Random Forest: A Case Study in Kansas, USA. *Remote Sens.* **2015**, *7*, 5347–5369. [CrossRef]
31. Zhang, L.; Liu, Z.; Liu, D.Y.; Xiong, Q.; Yang, N.; Ren, T.W.; Zhang, C.; Zhang, X.D.; Li, S.M. Crop Mapping Based on Historical Samples and New Training Samples Generation in Heilongjiang Province, China. *Sustainability* **2019**, *11*, 5052.
32. Blickensdorfer, L.; Schwieder, M.; Pflugmacher, D.; Nendel, C.; Erasmi, S.; Hostert, P. Mapping of crop types and crop sequences with combined time series of Sentinel-1, Sentinel-2 and Landsat 8 data for Germany. *Remote Sens. Environ.* **2022**, *269*, 112831. [CrossRef]
33. Tong, C.L.; Hall, C.A.S.; Wang, H.Q. Land use change in rice, wheat and maize production in China (1961–1998). *Agric. Ecosyst. Environ.* **2003**, *95*, 523–536. [CrossRef]
34. Wang, J.Y.; Zhang, Z.W.; Liu, Y.S. Spatial shifts in grain production increases in China and implications for food security. *Land Use Policy* **2018**, *74*, 204–213. [CrossRef]
35. Chen, C.Q.; van Groenigen, K.J.; Yang, H.Y.; Hungate, B.A.; Yang, B.; Tian, Y.L.; Chen, J.; Dong, W.J.; Huang, S.; Deng, A.X.; et al. Global warming and shifts in cropping systems together reduce China's rice production. *Glob. Food Secur.-Agric.* **2020**, *24*, 100359. [CrossRef]
36. Liu, Y.S.; Zhou, Y. Reflections on China's food security and land use policy under rapid urbanization. *Land Use Policy* **2021**, *109*, 105699. [CrossRef]
37. Olesen, J.E.; Trnka, M.; Kersebaum, K.C.; Skjelvag, A.O.; Seguin, B.; Peltonen-Sainio, P.; Rossi, F.; Kozyra, J.; Micale, F. Impacts and adaptation of European crop production systems to climate change. *Eur. J. Agron.* **2011**, *34*, 96–112. [CrossRef]
38. Liu, Y.Q.; Song, W. Modelling crop yield, water consumption, and water use efficiency for sustainable agroecosystem management. *J. Clean. Prod.* **2020**, *253*, 119940. [CrossRef]
39. Liu, Y.S.; Liu, X.Q.; Liu, Z.J. Effects of climate change on paddy expansion and potential adaption strategies for sustainable agriculture development across Northeast China. *Appl. Geogr.* **2022**, *141*, 102667. [CrossRef]
40. Liu, Z.J.; Yang, X.G.; Chen, F.; Wang, E.L. The effects of past climate change on the northern limits of maize planting in Northeast China. *Clim. Chang.* **2013**, *117*, 891–902. [CrossRef]
41. Dong, J.; Xiao, X.; Zhang, G.; Menarguez, M.A.; Choi, C.Y.; Qin, Y.; Luo, P.; Zhang, Y.; Moore, B. Northward expansion of paddy rice in northeastern Asia during 2000–2014. *Geophys. Res. Lett.* **2016**, *43*, 3754–3761. [CrossRef]
42. Yang, L.B.; Wang, L.M.; Huang, J.F.; Mansaray, L.R.; Mijiti, R. Monitoring policy-driven crop area adjustments in northeast China using Landsat-8 imagery. *Int. J. Appl. Earth Obs. Geoinf.* **2019**, *82*, 101982. [CrossRef]

43. Zhang, S.; Sun, L.; Jamshidi, A.H.; Niu, Y.; Fan, Z.; Zhang, H.; Liu, X. Assessment of the degree of sloped cropland degradation in typical black soil regions. *Land Degrad. Dev.* **2021**, *33*, 2220–2230. [CrossRef]
44. Yu, X.Y.; He, X.Y.; Zheng, H.F.; Guo, R.C.; Ren, Z.B.; Zhang, D.; Lin, J.X. Spatial and temporal analysis of drought risk during the crop-growing season over northeast China. *Nat. Hazards* **2014**, *71*, 275–289. [CrossRef]
45. Liu, X.B.; Zhang, X.Y.; Wang, Y.X.; Sui, Y.Y.; Zhang, S.L.; Herbert, S.J.; Ding, G. Soil degradation: A problem threatening the sustainable development of agriculture in Northeast China. *Plant Soil Environ.* **2010**, *56*, 87–97. [CrossRef]
46. Justice, C.O.; Townshend, J.R.G.; Vermote, E.F.; Masuoka, E.; Wolfe, R.E.; Saleous, N.; Roy, D.P.; Morisette, J.T. An overview of MODIS Land data processing and product status. *Remote Sens. Environ.* **2002**, *83*, 3–15. [CrossRef]
47. Liu, J.Y.; Kuang, W.H.; Zhang, Z.X.; Xu, X.L.; Qin, Y.W.; Ning, J.; Zhou, W.C.; Zhang, S.W.; Li, R.D.; Yan, C.Z.; et al. Spatiotemporal characteristics, patterns, and causes of land-use changes in China since the late 1980s. *J. Geogr. Sci.* **2014**, *24*, 195–210. [CrossRef]
48. Reuter, H.I.; Nelson, A.; Jarvis, A. An evaluation of void-filling interpolation methods for SRTM data. *Int. J. Geogr. Inf. Sci.* **2007**, *21*, 983–1008. [CrossRef]
49. Liu, F.; Wu, H.; Zhao, Y.; Li, D.; Yang, J.L.; Song, X.; Shi, Z.; Zhu, A.X.; Zhang, G.L. Mapping high resolution National Soil Information Grids of China. *Sci. Bull.* **2022**, *67*, 328–340. [CrossRef]
50. Heilongjiang Bureau of Statistics. *Heilongjiang Statistical Yearbook*; China Statistics Press: Beijing, China, 2001–2021.
51. Jilin Bureau of Statistics. *Jilin Statistical Yearbook*; China Statistics Press: Beijing, China, 2001–2021.
52. Liaoning Bureau of Statistics. *Liaoning Statistical Yearbook*; China Statistics Press: Beijing, China, 2001–2021.
53. Defries, R.S.; Townshend, J.R.G. Ndvi-Derived Land-Cover Classifications at a Global-Scale. *Int. J. Remote Sens.* **1994**, *15*, 3567–3586. [CrossRef]
54. Huete, A.; Didan, K.; Miura, T.; Rodriguez, E.P.; Gao, X.; Ferreira, L.G. Overview of the radiometric and biophysical performance of the MODIS vegetation indices. *Remote Sens. Environ.* **2002**, *83*, 195–213. [CrossRef]
55. Gao, B.C. NDWI—A normalized difference water index for remote sensing of vegetation liquid water from space. *Remote Sens. Environ.* **1996**, *58*, 257–266. [CrossRef]
56. Xiao, X.M.; Boles, S.; Liu, J.Y.; Zhuang, D.F.; Frolking, S.; Li, C.S.; Salas, W.; Moore, B. Mapping paddy rice agriculture in southern China using multi-temporal MODIS images. *Remote Sens. Environ.* **2005**, *95*, 480–492. [CrossRef]
57. Qi, J.; Marsett, R.; Heilman, P.; Bieden-bender, S.; Moran, S.; Goodrich, D.; Weltz, M. RANGES improves satellite-based information and land cover assessments in southwest United States. *Eos Trans. Am. Geophys. Union* **2002**, *83*, 601–606. [CrossRef]
58. van Deventer, A.P.; Ward, A.D.; Gowda, P.H.; Lyon, J.G. Using thematic mapper data to identify contrasting soil plains and tillage practices. *Photogram. Eng. Remote Sens.* **1997**, *63*, 87–93.
59. Gitelson, A.A.; Vina, A.; Arkebauer, T.J.; Rundquist, D.C.; Keydan, G.; Leavitt, B. Remote estimation of leaf area index and green leaf biomass in maize canopies. *Geophys. Res. Lett.* **2003**, *30*, 1248. [CrossRef]
60. Qi, J.; Chehbouni, A.; Huete, A.R.; Kerr, Y.H.; Sorooshian, S. A Modified Soil Adjusted Vegetation Index. *Remote Sens. Environ.* **1994**, *48*, 119–126. [CrossRef]
61. Salomonson, V.V.; Appel, I. Estimating fractional snow cover from MODIS using the normalized difference snow index. *Remote Sens. Environ.* **2004**, *89*, 351–360. [CrossRef]
62. Haralick, R.M.; Shanmugam, K.; Dinstein, I. Textural Features for Image Classification. *IEEE Trans. Syst. Man Cybern.* **1973**, *6*, 610–621. [CrossRef]
63. Tachikawa, T.; Hato, M.; Kaku, M.; Iwasaki, A. Characteristics of ASTER GDEM version 2. In Proceedings of the 2011 IEEE International Geoscience and Remote Sensing Symposium, Vancouver, BC, Canada, 24–29 July 2011; pp. 3657–3660.
64. Yin, Z.; Zhang, J.H. Operator functional state classification using least-square support vector machine based recursive feature elimination technique. *Comput. Methods Prog. Biol.* **2014**, *113*, 101–115. [CrossRef]
65. Liu, Y.Q.; Lu, C.H. Quantifying Grass Coverage Trends to Identify the Hot Plots of Grassland Degradation in the Tibetan Plateau during 2000–2019. *Int. J. Environ. Res. Public Health* **2021**, *18*, 416. [CrossRef]
66. Hao, P.Y.; Di, L.P.; Zhang, C.; Guo, L.Y. Transfer Learning for Crop classification with Cropland Data Layer data (CDL) as training samples. *Sci. Total Environ.* **2020**, *733*, 138869. [CrossRef] [PubMed]
67. Behnke, G.D.; Zuber, S.M.; Pittelkow, C.M.; Nafziger, E.D.; Villamil, M.B. Long-term crop rotation and tillage effects on soil greenhouse gas emissions and crop production in Illinois, USA. *Agric. Ecosyst. Environ.* **2018**, *261*, 62–70. [CrossRef]
68. Jarecki, M.; Grant, B.; Smith, W.; Deen, B.; Drury, C.; VanderZaag, A.; Qian, B.D.; Yang, J.Y.; Wagner-Riddle, C. Long-term Trends in Corn Yields and Soil Carbon under Diversified Crop Rotations. *J. Environ. Qual.* **2018**, *47*, 635–643. [CrossRef] [PubMed]
69. Van Eerd, L.L.; Congreves, K.A.; Hayes, A.; Verhallen, A.; Hooker, D.C. Long-term tillage and crop rotation effects on soil quality, organic carbon, and total nitrogen. *Can. J. Soil Sci.* **2014**, *94*, 303–315. [CrossRef]
70. Su, S.L.; Zhou, X.C.; Wan, C.; Li, Y.K.; Kong, W.H. Land use changes to cash crop plantations: Crop types, multilevel determinants and policy implications. *Land Use Policy* **2016**, *50*, 379–389. [CrossRef]
71. Zheng, X.; Zhu, J.J.; Yan, Q.L.; Song, L.N. Effects of land use changes on the groundwater table and the decline of *Pinus sylvestris* var. mongolica plantations in southern Horqin Sandy Land, Northeast China. *Agric. Water Manag.* **2012**, *109*, 94–106. [CrossRef]
72. Nie, T.Z.; Zhang, Z.X.; Qi, Z.J.; Chen, P.; Sun, Z.Y.; Liu, X.C. Characterizing Spatiotemporal Dynamics of CH4 Fluxes from Rice Paddies of Cold Region in Heilongjiang Province under Climate Change. *Int. J. Environ. Res. Public Health* **2019**, *16*, 692. [CrossRef]

73. Yang, S.H.; Xiao, Y.N.; Sun, X.; Ding, J.; Jiang, Z.W.; Xu, J.Z. Biochar improved rice yield and mitigated CH4 and N2O emissions from paddy field under controlled irrigation in the Taihu Lake Region of China. *Atmos. Environ.* **2019**, *200*, 69–77. [CrossRef]
74. Liu, S.; Yang, J.Y.; Zhang, X.Y.; Drury, C.F.; Reynolds, W.D.; Hoogenboom, G. Modelling crop yield, soil water content and soil temperature for a soybean-maize rotation under conventional and conservation tillage systems in Northeast China. *Agric. Water Manag.* **2013**, *123*, 32–44. [CrossRef]